NeuroImage xxx (2010) xxx–xxx

Contents lists available at ScienceDirect

NeuroImage

journal homepage: www.elsevier.com/locate/ynimg

Maze training in mice induces MRI-detectable brain shape changes specific to the type of learning

Jason P. Lerch [a,b,c,*], Adelaide P. Yiu [c,d,e], Alonso Martinez-Canabal [c,d,e], Tetyana Pekar [c,d,e], Veronique D. Bohbot [f], Paul W. Frankland [c,d,e], R. Mark Henkelman [a,b], Sheena A. Josselyn [c,d,e], John G. Sled [a,b]

[a] Mouse Imaging Centre, Hospital for Sick Children, Toronto, Ontario, Canada
[b] Department of Medical Biophysics, University of Toronto, Toronto, Ontario, Canada
[c] Program in Neurosciences & Mental Health, Hospital for Sick Children, Toronto, Ontario, Canada
[d] Department of Physiology, University of Toronto, Toronto, Ontario, Canada
[e] Institute of Medical Sciences (IMS), University of Toronto, Toronto, Ontario, Canada
[f] Douglas, Department of Psychiatry, McGill University, Verdun, Quebec, Canada

ARTICLE INFO

Article history:
Received 27 July 2010
Revised 4 September 2010
Accepted 30 September 2010
Available online xxxx

ABSTRACT

Multiple recent human imaging studies have suggested that the structure of the brain can change with learning. To investigate the mechanism behind such structural plasticity, we sought to determine whether maze learning in mice induces brain shape changes that are detectable by MRI and whether such changes are specific to the type of learning. Here we trained inbred mice for 5 days on one of three different versions of the Morris water maze and, using high-resolution MRI, revealed specific growth in the hippocampus of mice trained on a spatial variant of the maze, whereas mice trained on the cued version were found to have growth in the striatum. The structure-specific growth found furthermore correlated with GAP-43 staining, a marker of neuronal process remodelling, but not with neurogenesis nor neuron or astrocyte numbers or sizes. Our findings provide evidence that brain morphology changes rapidly at a scale detectable by MRI and furthermore demonstrate that specific brain regions grow or shrink in response to the changing environmental demands. The data presented herein have implications for both human imaging as well as rodent structural plasticity research, in that it provides a tool to screen for neuronal plasticity across the whole brain in the mouse while also providing a direct link between human and mouse studies.

Introduction

A series of studies have recently shown that the shape of the brain changes with learning at a scale detectable by MRI in human subjects. Grey matter density increases in the occipital and/or parietal lobes in juggling (Draganski et al., 2004), matched by fractional anisotropy increases in the right hemisphere (Scholz et al., 2009). These changes are detectable as early as 7 days after training (Driemeyer et al., 2008) and appear to occur in elderly as well as young subjects (Boyke et al., 2008). Similarly, musical instrument lessons in young childhood alter brain development (Hyde et al., 2009), and adult musicians feature multiple anatomical differences compared to non music-playing controls (Schlaug, 2001; Gaser and Schlaug, 2003; Bermudez et al., 2009). There is, in addition to the MRI studies cited above, a wealth of literature studying the effects of learning on the brain in the rodent (see Markham and Greenough, 2004, for a review). Training induces rapid alterations in synapse morphology and dendritic spine numbers (Lendvai et al., 2000; Holtmaat et al., 2005; Lippman and Dunaevsky, 2005), axonal and dendritic branch remodelling (De Paola et al., 2006), neurogenesis (Christie and Cameron, 2006; Kee et al., 2007), and astrocyte morphology (Haber et al., 2006; Todd et al., 2006). The link between the macroscopic alterations seen in the human MRI studies and microscopic changes investigated to date in the rodent is, however, still missing. Here we propose that high-resolution MRI imaging of mice trained on spatial mazes can offer this crucial link. The mouse makes for an excellent model organism to study brain plasticity, foremost due to the rich set of tools to manipulate its genome along with a plethora of extant mouse models relevant to brain plasticity research. Its small size, however, presents a challenge for MRI, which can be partially compensated for by increasing the scan time or using fixed specimens along with MR contrast agents to obtain exquisite resolution. We used the latter approach to scan fixed brains at 32-μm isotropic resolution for this study, with three specimens scanned simultaneously with independent transmit/receive coils to allow for adequate throughput (Bock et al., 2005; Nieman et al., 2005, 2007). Anatomical measures obtained from these fixed specimens have been used in multiple phenotyping studies (Chen et al., 2005; Clapcote et al., 2007; Spring et al., 2007; Lerch et al., 2008a,b; Mercer

* Corresponding author. Mouse Imaging Centre, The Hospital for Sick Children, 25 Orde St., Toronto, Ontario, Canada M5T 3H7.
E-mail address: jason@phenogenomics.ca (J.P. Lerch).

1053-8119/$ – see front matter © 2010 Elsevier Inc. All rights reserved.
doi:10.1016/j.neuroimage.2010.09.086

et al., 2009; Ellegood et al., 2010; Yu et al., 2010), and validated against stereology (Lerch et al., 2008b; Spring et al., 2010), where the MR measures were found to have greater sensitivity at discriminating between groups compared to classic tissue slice-based techniques (Lerch et al., 2008b).

To study the macroscopic effects of learning on the brain, we trained mice on a spatial learning paradigm. There is a direct human correlate to spatial learning: in 2000, Eleanor Maguire published an intriguing study which showed that London Taxi drivers have enlarged midposterior hippocampi compared to non-taxi driving controls (Maguire et al., 2000) and bus drivers (Maguire et al., 2006). These results, later expanded by further studies (Bohbot et al., 2007), suggested that employing a relational spatial navigation strategy (i.e., forming a cognitive map of the environment) over a non-relational response strategy (navigating by using simple landmark cues) was reflected by the volumes of different brain structures, in particular the striatum and hippocampus. We thus trained 2.5-month-old inbred mice on one of three versions of the Morris water maze (MWM, 6 trials a day for 5 days), wherein the animal must learn to navigate a novel environment in order to find a hidden platform. Navigation is thought to be supported by multiple, anatomically distinct systems that may interact in a co-operative or competitive fashion (McDonald and White, 1993; Poldrack and Packard, 2003). It is well established that spatial memory based navigation, which involves learning relationships between environmental landmarks, engages the hippocampus (O'Keefe and Nadel, 1978), also known to be involved in relational or declarative memory (Squire and Zola-Morgan, 1991; Eichenbaum et al., 1992). On the other hand, navigation relying on non-spatial 'response learning' involves the striatum (Packard et al., 1989; McDonald and White, 1993, 1994; Iaria et al., 2003), also known to be involved in procedural learning or habit formation (Squire and Butters, 1984). In using different variants of the MWM, we thus expected to be able to stimulate growth in the hippocampus and striatum selectively and furthermore take advantage of the whole brain coverage of MRI to assess for alterations outside these two key regions.

Methods

Mice

Male offspring (aged 2.5 months) from a cross between C57BL/6NTacfBr and 129Svev mice (Taconic Farms, Germantown, NY) were used in these experiments and housed in cage of 3–5 same-sex littermates. All animal experiments were approved by the animal ethics committee of the Hospital for Sick Children.

Water maze and general training procedures

Behavioural testing was conducted in a circular water maze pool (120 cm in diam.), located in a dimly lit room (see Teixeira et al., 2006, for details). The pool was filled with water (28 ± 1 °C) made opaque by a white nontoxic pigment. A circular escape platform (10 cm in diameter) was submerged 0.5 cm below the water surface and located in the one of the quadrants.

Mice, including home cage control mice, were handled for 2 min/day for 1 week before training began. On each training day, mice received six training trials (presented in two blocks of three trials; interblock interval was ~1 h; intertrial interval was ~15 s). The trial began by placing the mouse into the pool, facing the wall, in one of four pseudorandomly chosen start locations. The trial was complete once the mouse found the platform or 60 s had elapsed. If the mouse failed to find the platform on a given trial, the experimenter guided the mouse onto the platform.

We used three different water maze training protocols (see Fig. 1). In the spatial MWM version, the hidden platform was submerged in a fixed location for all trials and the perimeter of the experimental room had distinct visual landmarks. In the non-spatial cued MWM group version, the platform was marked by a visible cue (cylinder 4 cm diameter × 4 cm sitting on top of the platform) and moved to a different location on each trial. A black curtain surrounded the pool, obscuring the distal visual landmarks, to minimize reliance on spatial strategies. In the spatial cued MWM group version, a cued platform in a fixed location was used but with the distal visual landmarks visible, allowing for both the response as well as spatial memory strategies. Other types of control conditions have been used, including swimming controls (Gusev et al., 2005). However, whereas swimming controls equate swimming experience, reinforcement differs between groups and this may lead to differences in motivation and/or stress levels. Behavioural data from training and the probe tests were acquired and analysed using an automated tracking system (Actimetrics, Wilmette, IL). During training, we assessed the escape latency (time to reach the platform). Spatial memory was assessed in a 60-s probe test during which the platform was removed from the pool. We quantified performance by measuring the amount of time mice searched the target zone (20 cm in radius, centred on the location of the platform during training) versus the average of three other equivalent zones in other areas of the pool.

MR sample preparation

The first 32 mouse brains (6 controls, 6 non-spatial cued MWM (one data set discarded due to air bubbles in the parenchyma), 6 spatial cued MWM, and 14 spatial MWM) were prepared as follows. Ten days after the probe test, mice were anaesthetized (ketamine, 100 mg/kg and Rompun, 20 mg/kg, ip), perfused through the heart with phosphate buffered saline (PBS, 30 ml, pH 7.4, 25 °C) followed by paraformaldehyde (4% PFA; 30 ml, iced), as previously described (Tyszka et al., 2006). Bodies, along with the skin, lower jaw, ears, and the cartilaginous nose tip were removed. The remaining skull structures containing the brain were allowed to postfix in 4% PFA at 4 °C for 12 h. Following a washout period of 5 days in phosphate-buffered saline (PBS) and 0.01% sodium azide at 15 °C, the skulls were transferred to a PBS and 2 mM ProHance® (Bracco Diagnostics Inc., Princeton, NJ) solution for at least 7 days at 15 °C. MR imaging occurred 12 to 21 days post-mortem. A second set of 32 brains (6 controls, 9 non-spatial cued MWM, 9 spatial cued MWM, and 9 spatial MWM (one discarded due to air bubbles in the parenchyma)) were prepared in a slightly modified fashion to allow for follow-up histology. The mice were anaesthetized as above, also perfused through the heart with phosphate buffered saline (PBS, 30 ml, pH 7.4, 25 °C) followed by paraformaldehyde (4% PFA; 30 ml, iced) in PBS, but for these mice, a contrast agent (2 mM ProHance) was added at perfusion time. Bodies, along with the skin, lower jaw, ears, and the cartilaginous nose tip were then removed. The remaining skull structures containing the brain were allowed to postfix in 4% PFA plus 2 mM ProHance at 4 °C for 12 h. The skulls were then transferred to solution containing 1× PBS + 0.02% sodium azide + 2 mM ProHance for 4 days at 15 °C. MR imaging occurred 4 to 21 days post-mortem. We covaried for MR specimen preparation in all statistical analyses to assure that these differences did not influence our results.

MR acquisition

A multi-channel 7.0-T MRI scanner (Varian Inc., Palo Alto, CA) with a 6-cm inner bore diameter insert gradient was used to acquire anatomical images of brains within skulls. Before imaging, the samples were removed from the contrast agent solution, blotted and placed into plastic tubes (13 mm in diameter) filled with a proton-free susceptibility-matching fluid (Fluorinert FC-77, 3 M Corp., St. Paul, MN). Three custom-built, solenoid coils (14 mm in diameter, 18.3 cm in length) with over wound ends were used to image three brains in parallel. Parameters used in the scans were optimized for

Please cite this article as: Lerch, J.P., et al., Maze training in mice induces MRI-detectable brain shape changes specific to the type of learnin..., NeuroImage (2010), doi:10.1016/j.neuroimage.2010.09.086

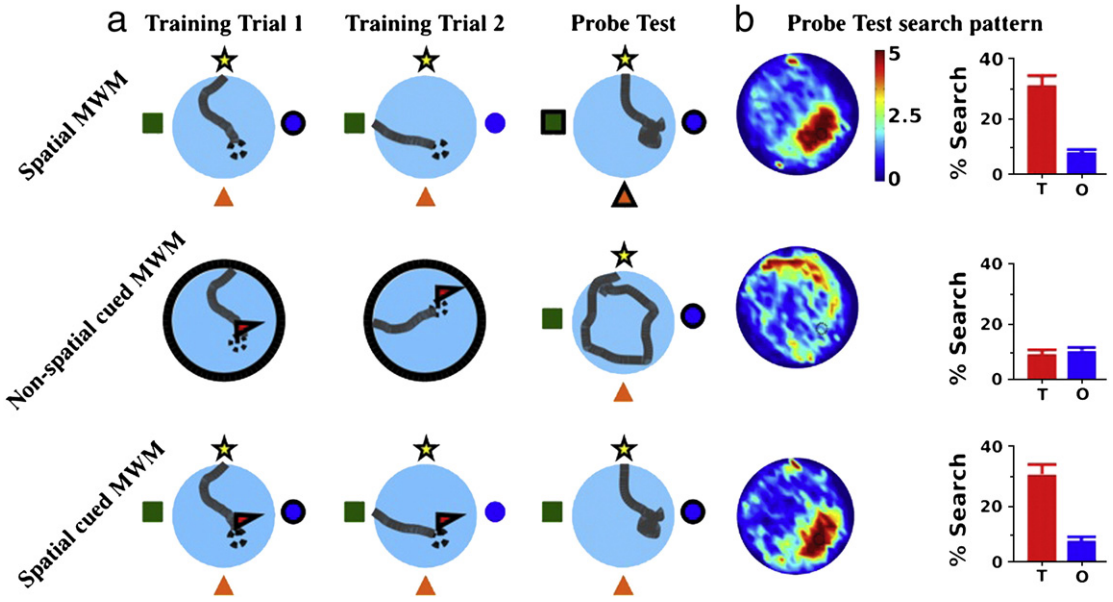

Fig. 1. Experimental design and spatial memory test. (a) Experimental design, showing the distal visual landmarks present in the spatial MWM and spatial cued MWM versions of the task, and the cued platform used for the non-spatial cued MWM and spatial cued MWM mice. The platform moved between trials for the non-spatial cued MWM mice, but remained in the same place for the other two MWM groups. (b) Left, density plots for grouped data, showing where mice concentrated their searches in the probe test (colour scale represents the number of visits per mouse per 5 cm × 5 cm area). Right, in the probe test, mice trained with visual landmarks spent more time searching the target zone (T, red) compared with other (O, blue) zones than did the mice trained on the non-spatial cued MWM (all $P<0.01$; paired t-tests).

grey/white matter contrast: a T2-weighted, 3D fast spin-echo sequence with 6 echoes, with TR/TE = 325/32 ms, four averages, field-of-view $14\times14\times25$ mm^3, and matrix size $=432\times432\times780$ giving an image with 32 μm isotropic voxels. Total imaging time was 11.3 h (Spring et al., 2007). Geometric distortion due to position of the three coils inside the magnet was calibrated using a precision machined MR phantom.

MR image analysis

We used an image registration-based approach to assess anatomical differences related to MWM training regimen. Image registration finds a smooth spatial transformation that best aligns one image to another such that corresponding anatomical features are superimposed. The deformation (local expansion, contraction, rotations, and translations) that brings the two into alignment thus becomes a summary of how they differ. We used an automated intensity-based group-wise registration approach (Collins et al., 1994, 1995; Kovacević et al., 2005) to align all brains in the study into a common coordinate system, yielding an average image of all brains and deformations that relate individual images to this average. The final deformation fields were computed with a greedy symmetric diffeomorphic registration (the SyN algorithm in ANTS (Avants et al., 2008; Klein et al., 2009)), then inverted and blurred with a 100-μm gaussian smoothing kernel and the Jacobian determinants of these deformations extracted, giving us a measure of local volume expansion/contraction at every point in the brain. An ANOVA was then computed at every voxel relating this expansion/contraction factor against MWM training regimen. Multiple comparisons were controlled for using the false discovery rate (Genovese et al., 2002). In addition, an anatomical atlas labelled with 62 distinct structures (Dorr et al., 2008) was used to compute volumes of each structure for each mouse.

Immunohistochemistry

Following MR imaging, the 32 fixed brains processed with the short MR sample preparation protocol were removed from the skull and paraffin embedded. About 4–8 consecutive 5-μm coronal slices per stain were taken through the hippocampus/dentate gyrus as well as the striatum. Sections were stained with either mouse anti-NeuN (neuronal nuclei, 1:100; Chemicon), rabbit anti-GAP-43 (growth-associated protein 43, 1:100; Abcam), or rabbit anti-GFAP (glial fibrillary acidic protein, 1:100; SIGNET). A further ten 5-μm coronal slices were acquired through the dentate gyrus and stained for DCX (double-cortin, 1:1000; Cell Signalling). For NeuN, GFAP, and GAP-43, quantification proceeded by first digitizing the slides using a slide scanner at 40× resolution. The dentate gyrus, CA1 and CA3 regions of the hippocampus, and striatum were then manually outlined on the digitized slides while blinded to their provenance. A neural net classifier (Zijdenbos et al., 2002) was then trained to discriminate between active stain (NeuN, GFAP, or GAP-43), counterstain (4′,6-diamidino-2-phenylindole, DAPI; the counterstain was used to aid in anatomical localization of each slice), and background, and the same classification rules were applied to every single slide of the same stain henceforth to ensure completely unbiased, quantitative results. The proportion of pixels stained by the active stain was the measure used for subsequent analyses (see Fig. 2). For the DCX stain, the total number of immunoreactive cells per slice was quantified by a blinded observer and the total surface of the granular cell layer of the hippocampus measured, therefore reporting the density of cells per tissue area.

Statistical analysis

The Jacobian determinant of the deformation fields, which provides an index of voxel expansion and contraction, was computed at every voxel (Chung et al., 2001). An ANOVA testing for a main effect of group with $F_{(3,59)}$ degrees of freedom was computed after covarying for differences in specimen preparation. The same ANOVA was computed to determine differences in anatomical structure volumes. To assess any correlations with behavioural outcomes, time spent searching the correct quadrant was correlated against structure volumes as well as Jacobian determinants in the spatial MWM group only. Multiple comparisons were thresholded using the false

Please cite this article as: Lerch, J.P., et al., Maze training in mice induces MRI-detectable brain shape changes specific to the type of learnin..., NeuroImage (2010), doi:10.1016/j.neuroimage.2010.09.086

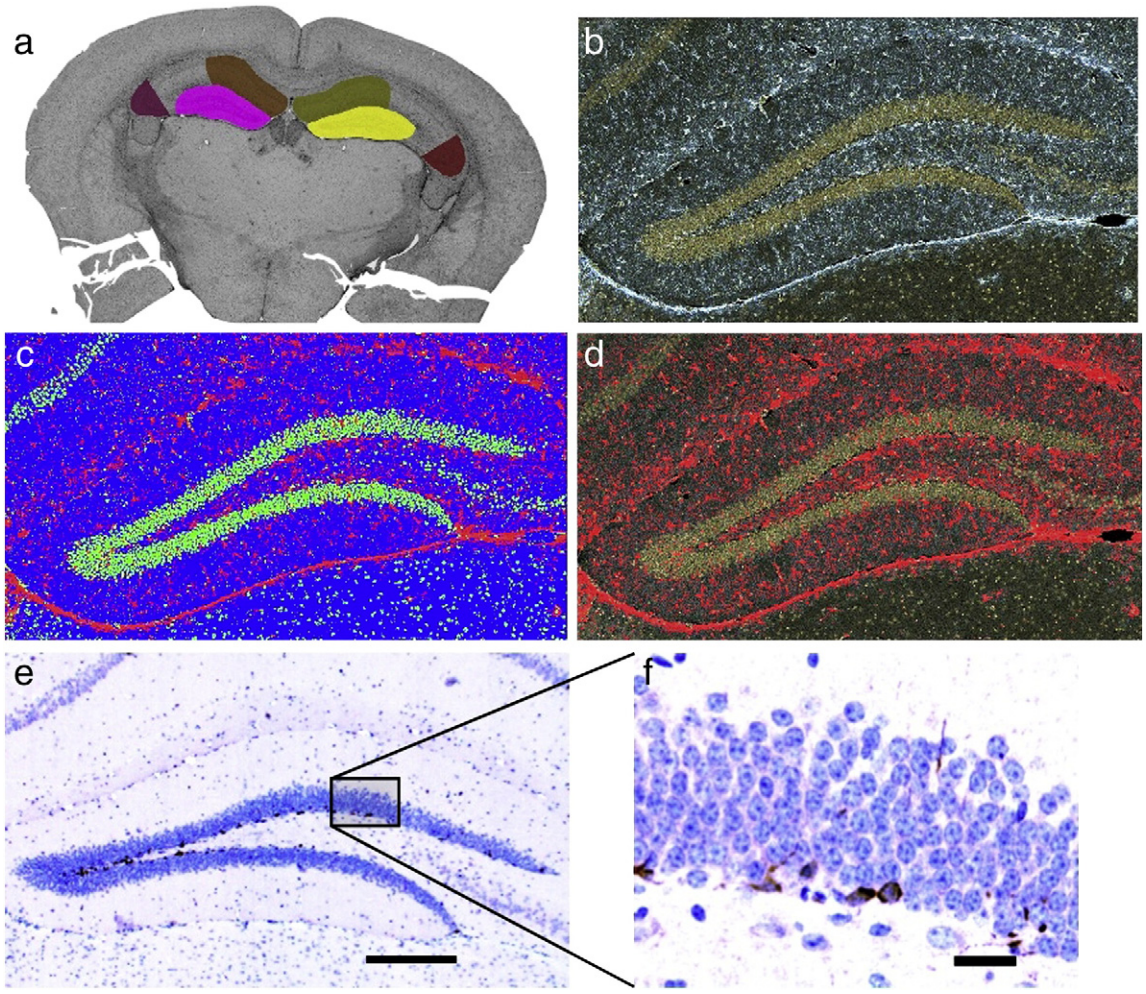

Fig. 2. IHC methods. To extract quantitative information from the immunohistochemistry, a low-resolution digitized slice was segmented into different hippocampal regions (a) and the striatum (not shown), the high-resolution data extracted (b, example from dentate gyrus with GFAP stain), classified into active stain (red), counter stain (DAPI, green), and background (blue). Just the active stain was retained (d), and a proportion of pixels for each anatomical structure were computed. For the DCX stain, the total number of immunoreactive cells per slice was quantified by a blinded observer (e and f).

discovery rate (Genovese et al., 2002) at 5% threshold. Mixed effects models with random intercepts per mouse were used for the correlations between immunohistochemistry staining and MRI based volumes. All errors given are standard errors of the mean and all confidence regions are 95% bootstrapped confidence intervals.

Results

Three versions of the MWM that differed with respect to cognitive demand were used. In the spatial MWM group, mice ($n=22$) were trained to find a hidden platform in a fixed location by using visual landmarks located around the room, a task requiring the hippocampus (Morris et al., 1982; McDonald and White, 1994). Alternatively, in the non-spatial cued MWM group ($n=14$), the platform was marked with a visible cue and located in a different position for each trial. The distal visual landmarks around the room were obscured for this task by a black curtain such that mice could not rely on a spatial strategy to find the platform, but instead had to engage a non-relational response strategy, reliant on the striatum (McDonald and White, 1994). A final group of mice ($n=15$) was trained on a spatial cued version of the MWM (a visibly cued platform in a fixed location with the distal visual landmarks in the room visible).

All mice showed evidence of learning as measured by a progressive decrease in latency to reach the platform following blocks of training trials. However, only mice trained with the spatial MWM and spatial cued MWM showed spatial memory on a subsequent probe test as they spent more time in the target zone, where the platform had been previously located (see Fig. 1). In contrast, mice trained in the non-spatial cued MWM searched randomly, indicating a lack of spatial memory, as per our prediction. Although mice trained under either protocol showed learning, the content of the learning differed. Importantly, there was no difference in exercise (distance travelled per day) between the spatial cued MWM and non-spatial cued MWM mice, whereas mice trained on the spatial MWM (the most challenging version of the maze) swam for significantly greater distances (see Fig. 3).

Navigation training causes neuroanatomical volume changes

The primary hypothesis was that mice trained on the spatial MWM would show growth of the hippocampus, whereas mice trained on the non-spatial cued MWM would show striatal enlargement. As can be seen in Fig. 4, this was indeed the case, with spatial MWM mice showing a 3.1% increase in the hippocampus when compared to control mice, and non-spatial cued MWM mice featuring a 1.9% enlargement of the striatum. The spatial cued MWM mice showed volume changes resembling those of the spatial MWM group, with a 3.8% increase in hippocampal volume and no significant difference in

Please cite this article as: Lerch, J.P., et al., Maze training in mice induces MRI-detectable brain shape changes specific to the type of learnin..., NeuroImage (2010), doi:10.1016/j.neuroimage.2010.09.086

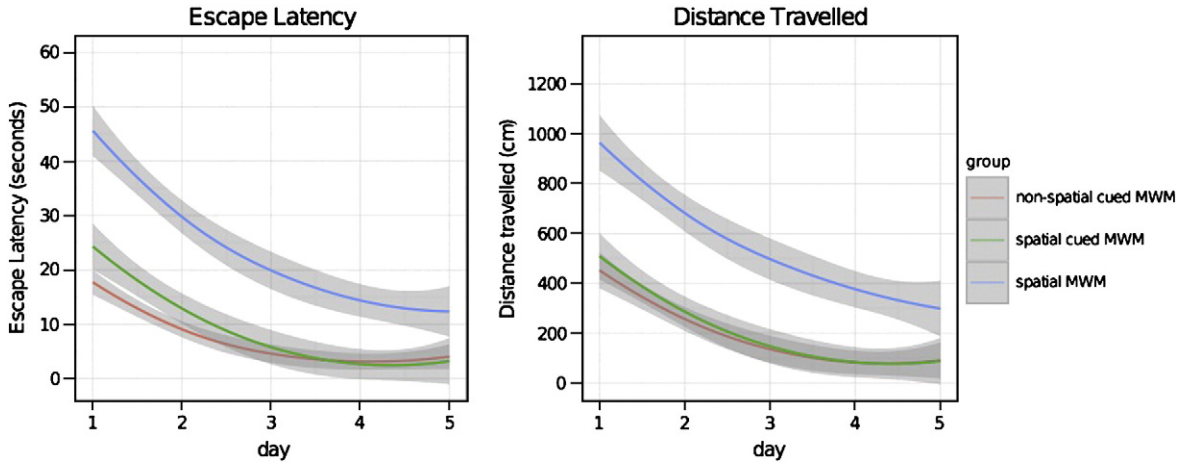

Fig. 3. Behavioural outcome. Two plots illustrate the learning trajectories of the three trained groups. In each case the spatial MWM mice travelled more and had a longer escape latency, whereas the spatial cued MWM and non-spatial cued MWM mice were similar or indistinguishable. Grey shaded regions illustrate 95% bootstrapped confidence intervals.

the striatum. When the search was extended to the rest of the brain, additional significant volume changes were detected in the corpus callosum, dentate gyrus of the hippocampus, internal capsule, cerebellum, frontal lobes, and entorhinal cortex; see Table 1 for a summary.

Along with the volume changes described above, local differences were determined at every voxel via a by-group ANOVA on the log Jacobian determinant of the deformation field. The resulting maps can be seen in Fig. 5; they show the same pattern of hippocampal enlargement in the two groups of mice with access to distal spatial cues along with striatal growth in the non-spatial cued MWM group. All trained mice appear to have enlarged dentate gyri (also detectable when examining structure volumes), and the spatial learning effects are primarily localized in areas CA1 and small parts of CA3 of the hippocampus. To account for any potential exercise confound, we compared just the two exercise matched groups, the non-spatial cued MWM and spatial cued MWM mice, and found that the key differences in the striatum and CA1 remained (Fig. 6).

Lastly, we correlated behavioural outcomes as measured by the probe trial against anatomical volumes as well as per-voxel Jacobian determinants. Given the differences in performance between groups and that *non-spatial cued MWM* mice are expected to search randomly, these correlations were limited to mice trained on the *spatial MWM* only. While trends towards increases in volume associated with better performance emerged in the hippocampal formation along with inverse correlations between performance and regions of the striatum and frontal cortices, none of these correlations survived correction for multiple comparisons.

MRI-detectable volume changes correlate with neuronal process remodelling

To understand the cellular bases of these localized volume changes, we examined four possible cellular hypotheses to account for the volume changes: (1) alterations in neuron numbers/sizes, (2) alterations in astrocyte numbers/sizes, (3) increased neurogenesis/survival of new neurons, and (4) remodelling of neuronal processes. Slices through the hippocampus and striatum were thus stained for NeuN, GFAP, DCX, and GAP-43, respectively. GAP-43 staining alone correlated positively with performance on the probe trial in the hippocampus ($p = 0.005$) but not in the dentate gyrus or striatum. We furthermore detected a significant positive correlation between GAP-43 and structure volume ($p = 0.000003$) but found no correlation between MR volume and any other IHC measure (DCX: $p = 0.4$; NeuN: $p = 0.66$; GFAP: $p = 0.67$; see

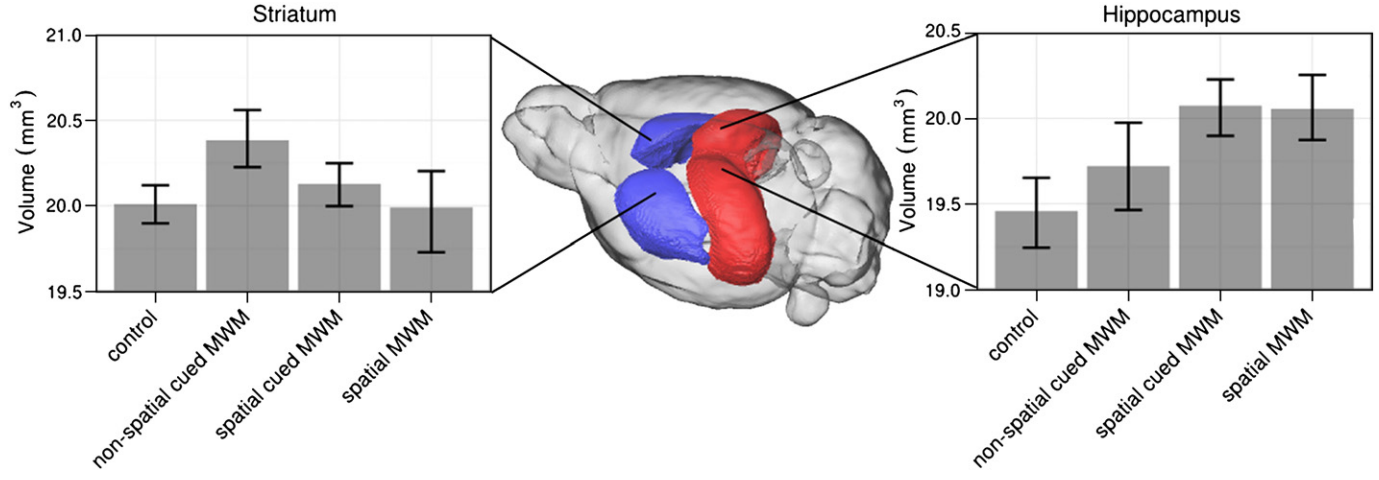

Fig. 4. Volumes of the hippocampus and striatum. The two plots show the volumes of the hippocampus and striatum; error bars represent 95% bootstrapped confidence intervals. The increase in volume of the striatum for the non-spatial cued MWM group and of the hippocampus for the spatial MWM and spatial cued MWM groups are readily apparent.

Please cite this article as: Lerch, J.P., et al., Maze training in mice induces MRI-detectable brain shape changes specific to the type of learnin..., NeuroImage (2010), doi:10.1016/j.neuroimage.2010.09.086

Table 1
Structure volume differences by water maze training regimen. An ANOVA was computed relating training group to structure volume, and the $F_{(3,59)}$ and q value (FDR-adjusted p value) retained. In addition, the percentage difference from the control group are shown for the three trained groups of mice, marked with an asterisk (*) if that difference is significant at a $p<0.05$ level (uncorrected), two asterisks (**) for $p<0.01$, and three asterisks (***) for $p<0.001$. Significant differences between each trained group and controls are only indicated if the main group effect was significant at an FDR of 10%.

Structure	$F_{(3,59)}$	q value	Non-spatial cued MWM (%)	Spatial cued MWM (%)	Spatial MWM (%)
Corpus callosum	7.94	0.004	1.52 ± 0.48**	0.33 ± 0.47	−0.49 ± 0.44
Dentate gyrus of hippocampus	7.22	0.004	2.6 ± 0.88**	3.8 ± 0.86***	3.08 ± 0.8***
Hippocampus	6.86	0.004	1.36 ± 0.86	3.17 ± 0.85***	3.08 ± 0.79***
Internal capsule	5.65	0.011	2.01 ± 0.77*	1.02 ± 0.76	−0.58 ± 0.7
Arbor vita of cerebellum	4.50	0.032	−1.48 ± 0.84	−0.41 ± 0.83	1.13 ± 0.77
Cerebral cortex: parietotemporal lobe	4.37	0.032	1 ± 0.74	−0.78 ± 0.73	−1.23 ± 0.68
Cerebral cortex: frontal lobe	3.98	0.043	0.26 ± 0.77	−0.97 ± 0.75	−1.78 ± 0.7*
Cerebellar cortex	3.44	0.063	−1.38 ± 0.69*	−0.67 ± 0.68	0.44 ± 0.63
Cerebral cortex: entorhinal cortex	2.89	0.095	−0.24 ± 0.94	1.42 ± 0.93	1.79 ± 0.86*
striatum	2.84	0.095	1.87 ± 0.82*	0.59 ± 0.81	−0.1 ± 0.75
Colliculus: inferior	1.59	0.360	0.96 ± 0.9	−0.08 ± 0.89	−0.75 ± 0.82
Nucleus accumbens	1.62	0.360	0.95 ± 0.81	1.46 ± 0.8	1.53 ± 0.74
Olfactory bulbs	1.53	0.360	0.04 ± 0.63	0.71 ± 0.62	0.99 ± 0.58
Amygdala	1.39	0.373	1.81 ± 0.97	1.61 ± 0.95	1.34 ± 0.88
Basal forebrain	1.42	0.373	0.45 ± 0.98	1.59 ± 0.96	1.48 ± 0.89
Olfactory tubercle	1.31	0.390	1.27 ± 1.14	2.21 ± 1.13	1.42 ± 1.04
Colliculus: superior	1.03	0.506	0.02 ± 0.63	0.92 ± 0.62	0.27 ± 0.58
Cerebral cortex: occipital lobe	0.89	0.536	−0.43 ± 0.89	0.82 ± 0.88	0.53 ± 0.81
Thalamus	0.92	0.536	−0.68 ± 0.81	−0.43 ± 0.8	0.4 ± 0.74
Periaqueductal grey	0.63	0.678	0.05 ± 0.73	0.67 ± 0.72	−0.16 ± 0.67
Hypothalamus	0.48	0.761	−0.23 ± 0.62	−0.57 ± 0.61	−0.59 ± 0.57
Fimbria	0.22	0.883	0.36 ± 1	0.27 ± 0.98	0.7 ± 0.91

Fig. 7). GAP-43 has been previously implicated in memory storage and, by binding to actin and fodrin, is believed to cause morphological change at presynaptic terminals through protein–protein interactions (Routtenberg et al., 2000). We can thus conclude that the largest explanatory factor for the MRI-detectable volume changes is the remodelling of neuronal processes.

Discussion

Learning causes neuroanatomical volume changes

There is strong evidence that laboratory mice kept in the same environment have remarkably similar brain anatomy (Chen et al., 2005). Therefore, the null hypothesis is that there will be no differences between mice trained on the three versions of the MWM. The regional volume increases and decreases that are specific to the training regimen in our study thus provides strong evidence for a causal relationship between training and resulting neuroanatomical changes, as per our hypotheses. These effects are specific to the learning paradigm and not determined by external factors such as exercise.

After training mice on different variants of the MWM, we found that 5 days of 6 trials per day were sufficient to grow the hippocampus by 3% to 4% if the mice used a spatial memory strategy to find the escape platform, and to conversely grow the striatum if the mice were forced to use a response strategy. The importance of the hippocampus and striatum in spatial and response learning respectively has been well established (McDonald and White, 1994; Devan et al., 1996; Korol and Kolo, 2002; Colombo et al., 2003; Gold, 2003; Hartley et al., 2003; Iaria et al., 2003; Bohbot et al., 2007; Doeller et al., 2008), showing that they change rapidly in volume due to learning is novel. Previous human imaging studies on navigation found that the sizes of anatomical structures differed between groups that had repeatedly used either a non-spatial/response or spatial navigation strategy, although a causal relationship was not established (Maguire et al., 2000, 2006; Bohbot et al., 2007). The results presented here, along with evidence that learning new tasks such as juggling (Draganski et al., 2004; Scholz et al., 2009) or playing musical instruments (Bermudez et al., 2009; Hyde et al., 2009) can alter neuroanatomy in humans, suggest that the size differences in the striatum and hippocampus found by Maguire et al. (2000, 2006) and size differences in the hippocampus and caudate nucleus of the striatum in Bohbot et al. (2007) were caused by the employment of one navigation strategy over the other.

In addition to the hypothesized hippocampal and striatal findings, the whole brain coverage provided by MRI allowed us to identify other regions that changed in volume in a task dependent manner. All trained mice had an enlarged dentate gyrus when compared to controls; this change is possibly related to general effects of enrichment and exercise previously associated with the dentate gyrus (Van Praag et al., 1999; Brown et al., 2003; Olson et al., 2006). White matter structures, such as the corpus callosum and internal capsule, were enlarged in the non-spatial cued MWM group, and the entorhinal cortex was increased by 1.8% in spatial MWM group. While we predominantly found volume increases, a few regions of volume decrease were also detected. As can be seen in Fig. 5, these decreases tend to occur in areas where another group shows concomitant increases, lending partial support to the competitive memory systems hypothesis (Packard et al., 1989; Packard and McGaugh, 1992; Poldrack and Packard, 2003). Intriguingly, the pattern of anatomical changes in the spatial cued MWM trained mice, which could use both a response strategy to travel to the flagged platform as well as rely on the distal spatial landmarks to form a cognitive map of the maze, was more similar to the spatial MWM mice than the non-spatial cued MWM group. These results suggest that, although the response strategy was available due to the flagged platform, young adult mice favour the spatial cognitive mapping strategy. These results are consistent with previous studies showing predominant use of spatial strategies in young adult rats tested on a "T" maze relative to older rodents who favour a response strategy (Barnes et al., 1980).

Learning to navigate a new environment increases the survival of new neurons in the dentate gyrus (Snyder et al., 2005; Christie and Cameron, 2006), the generation of dendritic spines (Lippman and Dunaevsky, 2005; Knott et al., 2006), the extension of dendrites, and the remodelling of astrocytic processes (Haber et al., 2006). Correlations with immunohistochemistry revealed that, among these

Please cite this article as: Lerch, J.P., et al., Maze training in mice induces MRI-detectable brain shape changes specific to the type of learnin..., NeuroImage (2010), doi:10.1016/j.neuroimage.2010.09.086

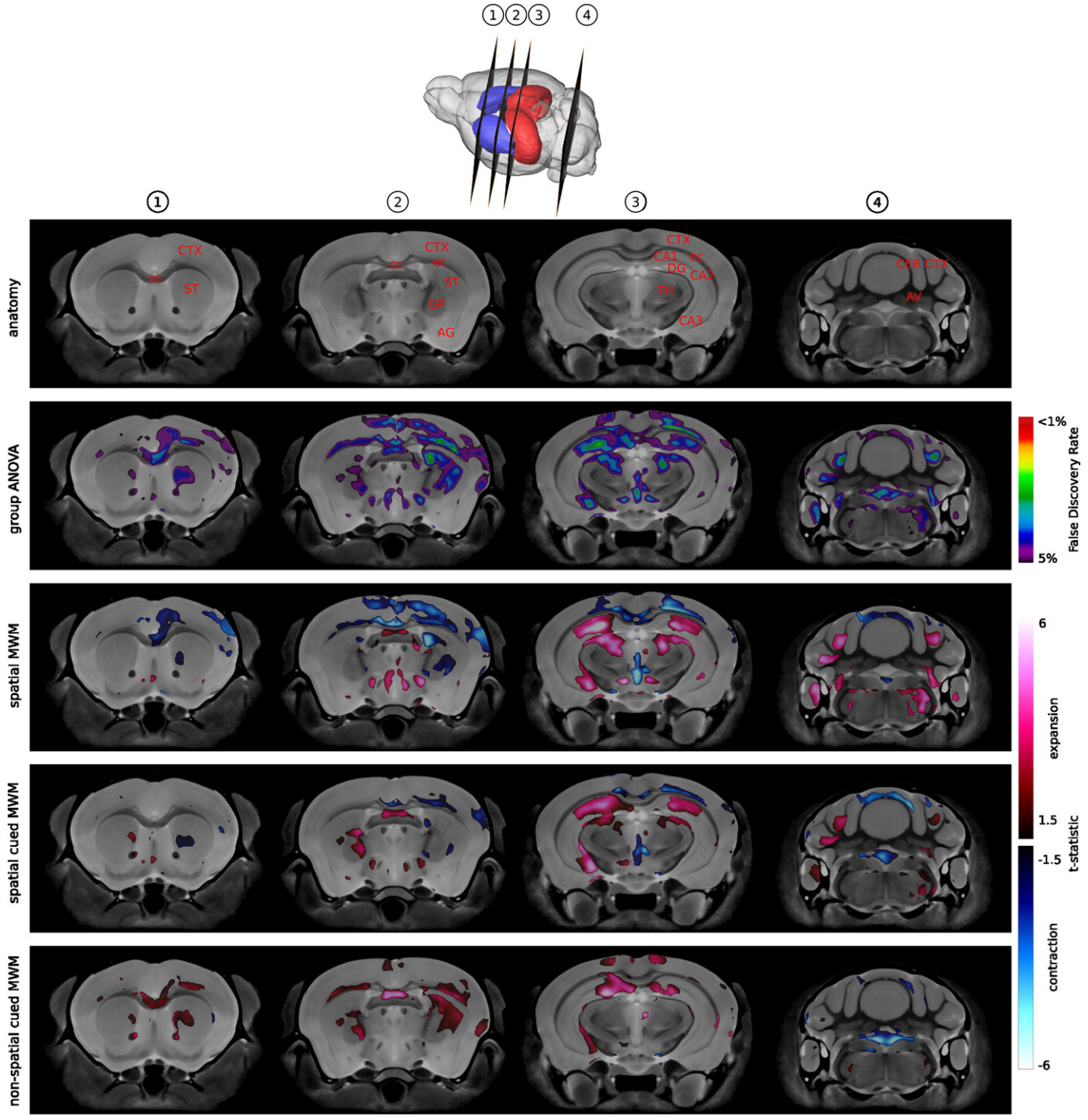

Fig. 5. Voxel-wise difference in local volume. The Jacobian determinant of the deformation field was computed and tested in an ANOVA to determine whether it differed by group; multiple comparisons were controlled using the false discovery rate. The first row provides anatomical labels: cc = corpus callosum, CTX = cortex, ec = external capsule, AG = amygdala, ST = striatum, GP = globus pallidus, DG = dentate gyrus, TH = thalamus, CER CTX = cerebellar cortex, AV = arbor vitae of the cerebellum. CA1, CA2, and CA3 refer to subdivisions of the hippocampus. The second row of images shows coronal slices with the level of significance colored. To assess the relative differences between the groups, a *t*-test was computed at every voxel comparing each trained group to the control mice. These *t*-tests were then masked by the ANOVA to retain only voxels where the ANOVA was significant at a 5% FDR; the results are shown in the bottom three panels, increases compared to controls displayed in red, decreases in blue.

different mechanisms, the remodelling of neuronal processes best accounts for the volume changes seen by MRI. GAP-43, the marker we used to assess process remodelling, targets presynaptic changes (Benowitz and Routtenberg, 1997; Routtenberg et al., 2000; Rekart et al., 2005; Holahan et al., 2007); the wealth of literature on axons and dendrites leads us to believe, however, that postsynaptic remodelling is occurring concurrently and at least as important to structural plasticity (Woolf, 1998; Engert and Bonhoeffer, 1999; Chklovskii et al., 2004; De Paola et al., 2006; Bourne and Harris, 2008). Differentiating which cellular components of neuronal plasticity

Please cite this article as: Lerch, J.P., et al., Maze training in mice induces MRI-detectable brain shape changes specific to the type of learnin..., NeuroImage (2010), doi:10.1016/j.neuroimage.2010.09.086

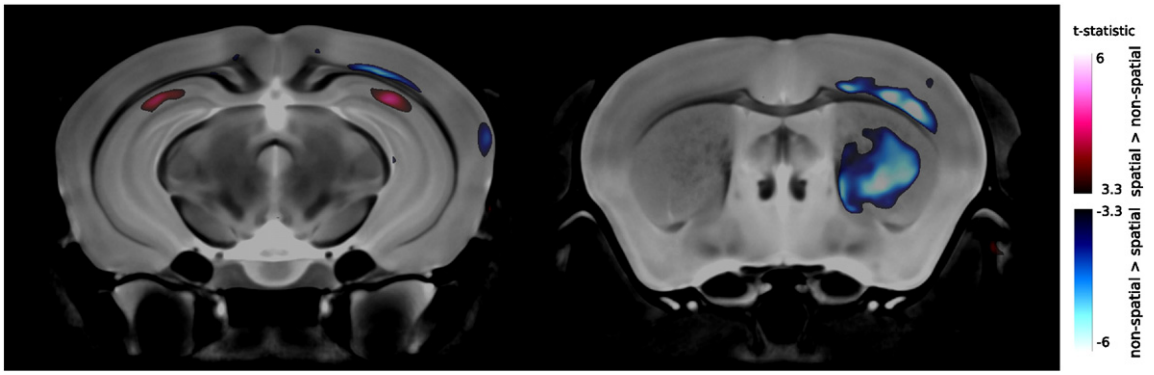

Fig. 6. Local volume differences after controlling for exercise. Given the differences in exercise between the four groups of mice, we repeated the local volume comparisons shown in Fig. 5 within just the spatial cued MWM and non-spatial cued MWM groups. As can be seen in Fig. 3, these two groups of mice do not differ in distance swum, and our probe trial data along with prior reports from the literature (Barnes et al., 1980) indicate that, despite the presence of a flagged platform, the spatial cued MWM mice still form a cognitive map of their environment. This figure thus shows that the volume changes in CA1 of the hippocampus as well as the right striatum are related to the cognitive strategy employed and not related to exercise confounds.

directly influence MR-detectable volume changes will be difficult using the type of correlational approach employed here and is thus beyond the scope of this paper; the use of different genetic mouse models will likely provide a more satisfying avenue for future investigations. At the moment, we can nevertheless confidently state that MR-detectable volume changes induced by learning are spatially correlated with neuronal process remodelling.

Structural MRI is capable of measuring the effects of experience on the brain

There is increasing evidence that neuroanatomy correlates with cognitive performance. Along with the spatial navigation findings of Maguire et al. (2000) and Bohbot et al. (2007) discussed above, Dickerson et al. (2008) found relationships between the thickness of the cortex and verbal memory in the medial temporal cortex and visuomotor speed in the parietal cortices. A complex interaction between IQ and cortical morphometry during adolescent development has also been identified (Shaw et al., 2006), and a study of twins revealed significant environmental components governing brain structure (Lenroot et al., 2009). Our results in mice trained on the water maze described above thus provide a platform for understanding how environment and learning can shape the brain in ways detectable in human as well as rodent studies.

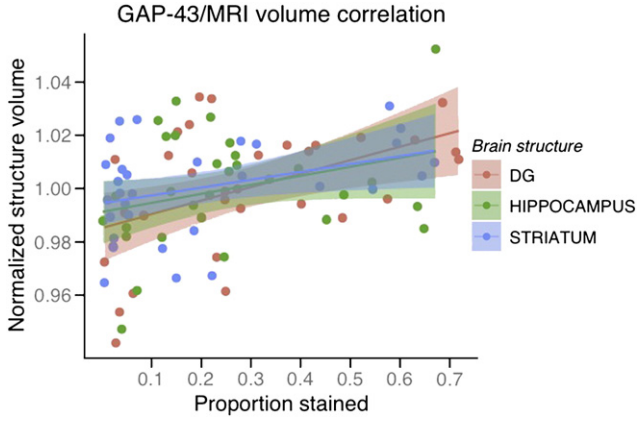

Fig. 7. Relation between GAP-43 and brain volume. This plot shows the correlation between proportion of pixels expressing GAP-43, an axonal growth cone marker, and MRI volume. The data is combined across three regions, with the MRI derived volume centred to the mean volume of all mice for each structure in order to allow all data to be shown on the same graph. The shaded regions represent 95% confidence intervals.

Implications for human imaging research

As mentioned above, there is growing evidence that training induces anatomical changes that can be observed in human imaging studies (Draganski et al., 2004; May and Gaser, 2006; May et al., 2006; Boyke et al., 2008; Driemeyer et al., 2008; Hyde et al., 2009; Scholz et al., 2009), although not all training studies found such a neuroanatomical signature (Thomas et al., 2009). Given that image acquisition and analysis using MRI can be kept comparable across species, studying the effects of training and learning in the mouse provides a tantalizing opportunity to better understand the cellular causes of the macroscopic changes seen by MRI. The tight genetic control afforded by the laboratory mouse provides remarkable precision for these types of experiments. The existence of multiple genetic mouse models of altered cellular processing and brain plasticity will, moreover, prove invaluable for establishing the sequence of events that underlie the effects of learning on the brain.

Implications for cellular plasticity research

Tremendous progress has recently been made in elucidating cellular aspects of structural brain plasticity (Kempermann et al., 1997; Engert and Bonhoeffer, 1999; Holtmaat et al., 2005; De Paola et al., 2006; Haber et al., 2006; Alvarez and Sabatini, 2007) in the rodent. The dominant methodologies behind these advances have been histology/immunohistochemistry (IHC), multi-photon microscopy, and electron microscopy (EM). However, these methods are limited to examining selected brain regions by technical limitations of field of view and skull window size (multi-photon) or the sheer labour needed to examine the whole brain (EM, IHC). Missing from the arsenal of brain plasticity research is a tool that allows one to rapidly search the entire brain to identify neuroanatomical regions undergoing plastic structural changes. Here we demonstrated that high-resolution MRI is capable of detecting neuroanatomical changes associated with learning. Mouse MRI can thus identify those regions undergoing structural plastic changes that may warrant further investigation using electron microscopy, immunohistochemistry, or multi-photon microscopy and that might otherwise be overlooked. While the numbers of mice we used were high, a simple power calculation shows that the kind of anatomical changes we saw (3%–4% in the hippocampus) could be recovered using 8 mice per group (at an α of 0.05, power of 0.8). To

Please cite this article as: Lerch, J.P., et al., Maze training in mice induces MRI-detectable brain shape changes specific to the type of learnin..., NeuroImage (2010), doi:10.1016/j.neuroimage.2010.09.086

conclude, we see MRI as especially useful for complex behavioural tasks where multiple brain regions could be affected as well as for the study of mutations where both the structural and functional characteristics of the brain can be altered.

Acknowledgements

The authors would like to thank Shoshana Spring and Christine Laliberte for their technical assistance; Ashu Jain and Dulcie Vousden for their assistance in delineating ROIs for the immunohistochemistry, and Dr. Robert Zatorre for insightful comments on the manuscript and experiment design. This research was supported by the Canadian Institutes of Health Research and the Ontario Research Fund.

References

Alvarez, V.A., Sabatini, B.L., 2007. Anatomical and physiological plasticity of dendritic spines. Annu. Rev. Neurosci. 30, 79–97.
Avants, B.B., Epstein, C.L., Grossman, M., Gee, J.C., 2008. Symmetric diffeomorphic image registration with cross-correlation: evaluating automated labeling of elderly and neurodegenerative brain. Med. Image Anal. 12, 26–41.
Barnes, C.A., Nadel, L., Honig, W.K., 1980. Spatial memory deficit in senescent rats. Can. J. Psychol. 34, 29–39.
Benowitz, L.I., Routtenberg, A., 1997. GAP-43: an intrinsic determinant of neuronal development and plasticity. Trends Neurosci. 20, 84–91.
Bermudez, P., Lerch, J.P., Evans, A.C., Zatorre, R.J., 2009. Neuroanatomical correlates of musicianship as revealed by cortical thickness and voxel-based morphometry. Cereb. Cortex 19, 1583–1596.
Bock, N., Nieman, B., Bishop, J., Mark Henkelman, R., 2005. In vivo multiple-mouse MRI at 7 Tesla. Magn. Reson. Med. 54, 1311–1316.
Bohbot, V., Lerch, J., Thorndycraft, B., Iaria, G., Zijdenbos, A., 2007. Gray matter differences correlate with spontaneous strategies in a human virtual navigation task. J. Neurosci. 27, 10078–10083.
Bourne, J.N., Harris, K.M., 2008. Balancing structure and function at hippocampal dendritic spines. Annu. Rev. Neurosci. 31, 47–67.
Boyke, J., Driemeyer, J., Gaser, C., Büchel, C., May, A., 2008. Training-induced brain structure changes in the elderly. J. Neurosci. 28, 7031–7035.
Brown, J., Cooper-Kuhn, C., Kempermann, G., Van Praag, H., Winkler, J., Gage, F., Kuhn, H., 2003. Enriched environment and physical activity stimulate hippocampal but not olfactory bulb neurogenesis. Eur. J. Neurosci. 17, 2042–2046.
Chen, X., Kovacevic, N., Lobaugh, N., Sled, J., Henkelman, R., Henderson, J., 2005. Neuroanatomical differences between mouse strains as shown by high-resolution 3D MRI. Neuroimage 7.
Chklovskii, D.B., Mel, B.W., Svoboda, K., 2004. Cortical rewiring and information storage. Nature 431, 782–788.
Christie, B., Cameron, H., 2006. Neurogenesis in the adult hippocampus. Hippocampus 16, 199–207.
Chung, M.K., Worsley, K.J., Paus, T., Cherif, C., Collins, D.L., Giedd, J.N., Rapoport, J.L., Evans, A.C., 2001. A unified statistical approach to deformation-based morphometry. Neuroimage 14, 595–606.
Clapcote, S., Lipina, T., Millar, J., Mackie, S., Christie, S., Ogawa, F., Lerch, J., Trimble, K., Uchiyama, M., Sakuraba, Y., 2007. Behavioral phenotypes of Disc1 missense mutations in mice. Neuron 54, 387–402.
Collins, D.L., Neelin, P., Peters, T.M., Evans, A.C., 1994. Automatic 3D intersubject registration of MR volumetric data in standardized Talairach space. J. Comput. Assist. Tomogr. 18, 192–205.
Collins, D., Holmes, C., Peters, T.M., Evans, A., 1995. Automatic 3-D model-based neuroanatomical segmentation. Hum. Brain Mapp. 3, 190–208.
Colombo, P.J., Brightwell, J.J., Countryman, R.A., 2003. Cognitive strategy-specific increases in phosphorylated cAMP response element-binding protein and c-Fos in the hippocampus and dorsal striatum. J. Neurosci. 23, 3547–3554.
De Paola, V., Holtmaat, A., Knott, G., Song, S., Wilbrecht, L., Caroni, P., Svoboda, K., 2006. Cell type-specific structural plasticity of axonal branches and boutons in the adult neocortex. Neuron 49, 861–875.
Devan, B.D., Goad, E.H., Petri, H.L., 1996. Dissociation of hippocampal and striatal contributions to spatial navigation in the water maze. Neurobiol. Learn. Mem. 66, 305–323.
Dickerson, B.C., Fenstermacher, E., Salat, D.H., Wolk, D.A., Maguire, R.P., Desikan, R., Pacheco, J., Quinn, B.T., van der Kouwe, A., Greve, D.N., Blacker, D., Albert, M.S., Killiany, R.J., Fischl, B., 2008. Detection of cortical thickness correlates of cognitive performance: reliability across MRI scan sessions, scanners, and field strengths. Neuroimage 39, 10–18.
Doeller, C., King, J., Burgess, N., 2008. Parallel striatal and hippocampal systems for landmarks and boundaries in spatial memory. Proc. Natl Acad. Sci. 105, 5915–5920.
Dorr, A., Lerch, J., Spring, S., Kabani, N., Henkelman, R., 2008. High resolution three-dimensional brain atlas using an average magnetic resonance image of 40 adult C57Bl/6J mice. Neuroimage 42, 60–69.
Draganski, B., Gaser, C., Busch, V., Schuierer, G., Bogdahn, U., May, A., 2004. Neuroplasticity: changes in grey matter induced by training. Nature 427, 311–312.
Driemeyer, J., Boyke, J., Gaser, C., Büchel, C., May, A., 2008. Changes in gray matter induced by learning—revisited. PLoS ONE 3, e2669.
Eichenbaum, H., Otto, T., Cohen, N.J., 1992. The hippocampus—what does it do? Behav. Neural Biol. 57, 2–36.
Ellegood, J., Pacey, L.K., Hampson, D.R., Lerch, J., Henkelman, R.M., 2010. Anatomical phenotyping in a mouse model of fragile X syndrome with magnetic resonance imaging. Neuroimage 53, 1023–1029.
Engert, F., Bonhoeffer, T., 1999. Dendritic spine changes associated with hippocampal long-term synaptic plasticity. Nature 399, 66–70.
Gaser, C., Schlaug, G., 2003. Brain structures differ between musicians and non-musicians. J. Neurosci. 23, 9240–9245.
Genovese, C.R., Lazar, N.A., Nichols, T., 2002. Thresholding of statistical maps in functional neuroimaging using the false discovery rate. Neuroimage 15, 870–878.
Gold, P., 2003. Acetylcholine modulation of neural systems involved in learning and memory. Neurobiol. Learn. Mem. 80, 194–210.
Gusev, P.A., Cui, C., Alkon, D.L., Gubin, A.N., 2005. Topography of Arc/Arg3.1 mRNA expression in the dorsal and ventral hippocampus induced by recent and remote spatial memory recall: dissociation of CA3 and CA1 activation. J. Neurosci. 25, 9384–9397.
Haber, M., Zhou, L., Murai, K., 2006. Cooperative astrocyte and dendritic spine dynamics at hippocampal excitatory synapses. J. Neurosci. 26, 8881–8891.
Hartley, T., Maguire, E., Spiers, H., Burgess, N., 2003. The well-worn route and the path less traveled: distinct neural bases of route following and wayfinding in humans. Neuron 37, 877–888.
Holahan, M., Honegger, K., Tabatadze, N., Routtenberg, A., 2007. GAP-43 gene expression regulates information storage. Learn. Mem. 14, 407–415.
Holtmaat, A., Trachtenberg, J., Wilbrecht, L., Shepherd, G., Zhang, X., Knott, G., Svoboda, K., 2005. Transient and persistent dendritic spines in the neocortex in vivo. Neuron 45, 279–291.
Hyde, K.L., Lerch, J., Norton, A., Forgeard, M., Winner, E., Evans, A., Schlaug, G., 2009. Musical training shapes structural brain development. J. Neurosci. 29, 3019–3025.
Iaria, G., Petrides, M., Dagher, A., Pike, B., Bohbot, V.D., 2003. Cognitive strategies dependent on the hippocampus and caudate nucleus in human navigation: variability and change with practice. J. Neurosci. 23, 5945–5952.
Kee, N., Teixeira, C.M., Wang, A.H., Frankland, P.W., 2007. Preferential incorporation of adult-generated granule cells into spatial memory networks in the dentate gyrus. Nat. Neurosci. 10, 355–362.
Kempermann, G., Kuhn, H.G., Gage, F.H., 1997. More hippocampal neurons in adult mice living in an enriched environment. Nature 386, 493–495.
Klein, A., Andersson, J., Ardekani, B.A., Ashburner, J., Avants, B., Chiang, M.C., Christensen, G.E., Collins, D.L., Gee, J., Hellier, P., Song, J.H., Jenkinson, M., Lepage, C., Rueckert, D., Thompson, P., Vercauteren, T., Woods, R.P., Mann, J.J., Parsey, R.V., 2009. Evaluation of 14 nonlinear deformation algorithms applied to human brain MRI registration. Neuroimage 46, 786–802.
Knott, G., Holtmaat, A., Wilbrecht, L., Welker, E., Svoboda, K., 2006. Spine growth precedes synapse formation in the adult neocortex in vivo. Nat. Neurosci. 9, 1117–1124.
Korol, D.L., Kolo, L.L., 2002. Estrogen-induced changes in place and response learning in young adult female rats. Behav. Neurosci. 116, 411–420.
Kovacević, N., Henderson, J.T., Chan, E., Lifshitz, N., Bishop, J., Evans, A.C., Henkelman, R.M., Chen, X.J., 2005. A three-dimensional MRI atlas of the mouse brain with estimates of the average and variability. Cereb. Cortex 15, 639–645.
Lendvai, B., Stern, E.A., Chen, B., Svoboda, K., 2000. Experience-dependent plasticity of dendritic spines in the developing rat barrel cortex in vivo. Nature 404, 876–881.
Lenroot, R., Schmitt, J., Ordaz, S., Wallace, G., Neale, M., Lerch, J., Kendler, K., Evans, A., Giedd, J., 2009. Differences in genetic and environmental influences on the human cerebral cortex associated with development during childhood and adolescence. Hum. Brain Mapp. 30, 163–174.
Lerch, J., Carroll, J., Dorr, A., Spring, S., Evans, A., Hayden, M., Sled, J., Henkelman, R., 2008a. Cortical thickness measured from MRI in the YAC128 mouse model of Huntington's disease. Neuroimage 41, 243–251.
Lerch, J., Carroll, J., Spring, S., Bertram, L., Schwab, C., Hayden, M., Markhenkelman, R., 2008b. Automated deformation analysis in the YAC128 Huntington disease mouse model. Neuroimage 39, 32–39.
Lippman, J., Dunaevsky, A., 2005. Dendritic spine morphogenesis and plasticity. J. Neurobiol. 64, 47–57.
Maguire, E.A., Gadian, D.G., Johnsrude, I.S., Good, C.D., Ashburner, J., Frackowiak, R.S., Frith, C.D., 2000. Navigation-related structural change in the hippocampi of taxi drivers. Proc. Natl Acad. Sci. USA 97, 4398–4403.
Maguire, E., Woollett, K., Spiers, H., 2006. London taxi drivers and bus drivers: a structural MRI and neuropsychological analysis. Hippocampus 16, 1091–1101.
Markham, J.A., Greenough, W.T., 2004. Experience-driven brain plasticity: beyond the synapse. Neuron Glia Biol. 1, 351–363.
May, A., Gaser, C., 2006. Magnetic resonance-based morphometry: a window into structural plasticity of the brain. Curr. Opin. Neurol. 19, 407–411.
May, A., Hajak, G., Ganssbauer, S., Steffens, T., Langguth, B., Kleinjung, T., Eichhammer, P., 2006. Structural brain alterations following 5 days of intervention: dynamic aspects of neuroplasticity. Cereb. Cortex 17, 205–210.
McDonald, R.J., White, N.M., 1993. A triple dissociation of memory systems: hippocampus, amygdala, and dorsal striatum. Behav. Neurosci. 107, 3–22.
McDonald, R.J., White, N.M., 1994. Parallel information processing in the water maze: evidence for independent memory systems involving dorsal striatum and hippocampus. Behav. Neural Biol. 61, 260–270.
Mercer, R.E., Kwolek, E.M., Bischof, J.M., van Eede, M., Henkelman, R.M., Wevrick, R., 2009. Regionally reduced brain volume, altered serotonin neurochemistry, and abnormal behavior in mice null for the circadian rhythm output gene Magel2. Am. J. Med. Genet. B Neuropsychiatr. Genet. 150B, 1085–1099.
Morris, R.G., Garrud, P., Rawlins, J.N., O'Keefe, J., 1982. Place navigation impaired in rats with hippocampal lesions. Nature 297, 681–683.

Please cite this article as: Lerch, J.P., et al., Maze training in mice induces MRI-detectable brain shape changes specific to the type of learnin..., NeuroImage (2010), doi:10.1016/j.neuroimage.2010.09.086

Nieman, B., Bock, N., Bishop, J., Chen, X.J., Sled, J., Rossant, J., Henkelman, R.M., 2005. Magnetic resonance imaging for detection and analysis of mouse phenotypes. NMR Biomed. 18, 447–468.
Nieman, B., Bishop, J., Dazai, J., Bock, N., Lerch, J., Feintuch, A., Chen, X.J., Sled, J., Henkelman, R.M., 2007. MR technology for biological studies in mice. NMR Biomed. 20, 291–303.
O'Keefe, J., Nadel, L., 1978. The Hippocampus as a Cognitive Map. Clarendon Press Oxford University Press, Oxford New York.
Olson, A., Eadie, B., Ernst, C., Christie, B., 2006. Environmental enrichment and voluntary exercise massively increase neurogenesis in the adult hippocampus via dissociable pathways. Hippocampus 16, 250–260.
Packard, M.G., McGaugh, J.L., 1992. Double dissociation of fornix and caudate nucleus lesions on acquisition of two water maze tasks: further evidence for multiple memory systems. Behav. Neurosci. 106, 439–446.
Packard, M.G., Hirsh, R., White, N.M., 1989. Differential effects of fornix and caudate nucleus lesions on two radial maze tasks: evidence for multiple memory systems. J. Neurosci. 9, 1465–1472.
Poldrack, R.A., Packard, M.G., 2003. Competition among multiple memory systems: converging evidence from animal and human brain studies. Neuropsychologia 41, 245–251.
Rekart, J.L., Meiri, K., Routtenberg, A., 2005. Hippocampal-dependent memory is impaired in heterozygous GAP-43 knockout mice. Hippocampus 15, 1–7.
Routtenberg, A., Cantallops, I., Zaffuto, S., Serrano, P., Namgung, U., 2000. Enhanced learning after genetic overexpression of a brain growth protein. Proc. Natl Acad. Sci. USA 97, 7657–7662.
Schlaug, G., 2001. The brain of musicians. A model for functional and structural adaptation. Ann. NY Acad. Sci. 930, 281–299.
Scholz, J., Klein, M.C., Behrens, T.E.J., Johansen-Berg, H., 2009. Training induces changes in white-matter architecture. Nat. Neurosci. 12, 1370–1371.
Shaw, P., Greenstein, D., Lerch, J., Clasen, L., Lenroot, R., Gogtay, N., Evans, A., Rapoport, J., Giedd, J., 2006. Intellectual ability and cortical development in children and adolescents. Nature 440, 676–679.
Snyder, J., Hong, N., Mcdonald, R., Wojtowicz, J., 2005. A role for adult neurogenesis in spatial long-term memory. Neuroscience 130, 843–852.
Spring, S., Lerch, J., Henkelman, R., 2007. Sexual dimorphism revealed in the structure of the mouse brain using three-dimensional magnetic resonance imaging. Neuroimage 35, 1424–1433.
Spring, S., Lerch, J., Wetzel, M.K., Evans, A., Henkelman, R.M., 2010. Cerebral asymmetries in 12-week-old C57Bl/6 J mice measured by magnetic resonance imaging. Neuroimage 50, 409–415.
Squire, L.R., Butters, N., 1984. Neuropsychology of Memory. Guilford Press, New York.
Squire, L.R., Zola-Morgan, S., 1991. The medial temporal lobe memory system. Science 253, 1380–1386.
Teixeira, C., Pomedli, S.R., Maei, H.R., Kee, N., Frankland, P., 2006. Involvement of the anterior cingulate cortex in the expression of remote spatial memory. J. Neurosci. 26, 7555–7564.
Thomas, A.G., Marrett, S., Saad, Z.S., Ruff, D.A., Martin, A., Bandettini, P.A., 2009. Functional but not structural changes associated with learning: an exploration of longitudinal voxel-based morphometry (VBM). Neuroimage 15, 117–125.
Todd, K., Serrano, A., Lacaille, J., Robitaille, R., 2006. Glial cells in synaptic plasticity. J. Physiol. Paris 99, 75–83.
Tyszka, J.M., Readhead, C., Bearer, E.L., Pautler, R.G., Jacobs, R.E., 2006. Statistical diffusion tensor histology reveals regional dysmyelination effects in the shiverer mouse mutant. Neuroimage 29, 1058–1065.
Van Praag, H., Christie, B.R., Sejnowski, T.J., Gage, F.H., 1999. Running enhances neurogenesis, learning, and long-term potentiation in mice. Proc. Natl Acad. Sci. USA 96, 13427–13431.
Woolf, N.J., 1998. A structural basis for memory storage in mammals. Prog. Neurobiol. 55, 59–77.
Yu, T., Li, Z., Jia, Z., Clapcote, S.J., Liu, C., Li, S., Asrar, S., Pao, A., Chen, R., Fan, N., Carattini-Rivera, S., Bechard, A.R., Spring, S., Henkelman, R.M., Stoica, G., Matsui, S., Nowak, N.J., Roder, J.C., Chen, C., Bradley, A., Yu, Y.E., 2010. A mouse model of Down syndrome trisomic for all human chromosome 21 syntenic regions. Hum. Mol. Genet. 19, 2780–2791.
Zijdenbos, A.P., Forghani, R., Evans, A., 2002. Automatic "pipeline" analysis of 3-D MRI data for clinical trials: application to multiple sclerosis. IEEE Trans. Med. Imaging 21, 1280–1291.

Please cite this article as: Lerch, J.P., et al., Maze training in mice induces MRI-detectable brain shape changes specific to the type of learnin..., NeuroImage (2010), doi:10.1016/j.neuroimage.2010.09.086